CRI-EMOA: A Pareto-Front Shape Invariant Evolutionary Multi-Objective Algorithm*

Jesús Guillermo Falcón-Cardona, Carlos A. Coello Coello
and Michael T.M. Emmerich

CINVESTAV-IPN (Evolutionary Computation Group), Computer Science Department,
Av. IPN No. 2508, Col. San Pedro Zacatenco, México D.F. 07300, MEXICO
Leiden Institute of Advanced Computer Science, Leiden University,
Niels Bohrweg 1 2333 CA, Leiden, The Netherlands
jfalcon@computacion.cs.cinvestav.mx
ccoello@cs.cinvestav.mx
m.t.m.emmerich@liacs.leidenuniv.nl

Abstract. The use of multi-objective evolutionary algorithms (MOEAs) that employ a set of convex weight vectors as search directions, as a reference set or as part of a quality indicator has been widely extended. However, a recent study indicates that these MOEAs do not perform very well when tackling multi-objective optimization problem (MOPs), having different Pareto front geometries. Hence, it is necessary to propose MOEAs whose good performance is not strongly depending on certain Pareto front shapes. In this paper, we propose a Pareto-front shape invariant MOEA that combines the individual effect of two indicator-based density estimators. We selected the weakly Pareto-compliant IGD^+ indicator to promote convergence and the Riesz s-energy indicator that leads to uniformly distributed point sets for the large class of rectifiable d-dimensional manifolds. Our proposed approach, called CRI-EMOA, is compared with respect to MOEAs that adopt convex weight vectors (NSGA-III, MOEA/D and MOMBI2) as well as to MOEAs not using this set of vectors (Δ_p-MOEA and GDE-MOEA) on MOPs belonging to the test suites DTLZ, $DTLZ^{-1}$, WFG and WFG^{-1}. Our experimental results show that CRI-EMOA outperforms the considered MOEAs, regarding the hypervolume indicator and the Solow-Polasky indicator, on most of the test problems and that its performance does not depend on the Pareto front shape of the problems.

Keywords: Multi-Objective Optimization, Quality Indicators, Multi-Indicator Density Estimation

* The first author acknowledges support from CONACyT and CINVESTAV-IPN to pursue graduate studies in Computer Science. The second author gratefully acknowledges support from CONACyT grant no. 2016-01-1920 (*Investigación en Fronteras de la Ciencia 2016*).

1 Introduction

In the last 30 years, Multi-Objective Evolutionary Algorithms (MOEAs), which are population-based and gradient-free metaheuristics, have arisen as a popular approach to solve problems that involve the simultaneous optimization of several, often conflicting, objective functions [1]. These are the so-called multi-objective optimization problems (MOPs). MOEAs employ the principles of natural evolution to drive a set of objective vectors towards the Pareto optimal front that represents the solution to a MOP. In this regard, solving a MOP involves finding the best possible trade-offs among its objectives. The particular set that yields the best possible trade-offs among the objectives is known as the Pareto Optimal Set ($\mathcal{P}^*$) and its image is known as the Pareto Optimal Front ($\mathcal{PF}^*$).

Currently, there are different strategies for designing MOEAs, such as the decomposition of a MOP into several single-objective optimization problems [2], the use of reference sets to guide the population towards the Pareto front [3], and the generation of selection mechanisms based on (unary) quality indicators[1] [4]. A wide variety of state-of-the-art MOEAs based on the previously indicated strategies employ a set of convex weight vectors as search directions for the decomposition, in a method to construct reference sets, or as part of the definition of a quality indicator. A vector $\boldsymbol{w} \in \mathbb{R}^m$ is a convex weight vector if $\sum_{i=1}^{m} w_i = 1$ and $w_i \geq 0$ for all $i = 1, \ldots, m$. These weight vectors lie on an $(m-1)$-simplex. However, Ishibuchi *et al.* [5] empirically showed that the use of convex weight vectors overspecializes MOEAs on MOPs whose Pareto fronts are strongly correlated to the simplex formed by such weight vectors. In other words, such MOEAs are unable to produce good results when tackling MOPs whose Pareto fronts are not highly coupled with the $(m-1)$-simplex. In consequence, more general MOEAs need to be designed to avoid this overspecialization on specific benchmark problems such as the DTLZ and the WFG test suites.

There are MOEAs that do not use in any of their mechanisms a set of convex weight vectors. An example is the Nondominated Sorting Genetic Algorithm II (NSGA-II) [6] which uses Pareto dominance[2] in its main selection mechanism and crowding distance as its second selection mechanism. However, the selection pressure of NSGA-II dilutes when tackling MOPs having four or more objective functions. Additionally, the crowding distance density estimator cannot produce evenly distributed Pareto fronts in high dimensionality. Another example is the $\mathcal{S}$ Metric Selection Evolutionary Multi-Objective Algorithm (SMS-EMOA) [7] which is a steady-state MOEA that replaces the crowding distance of NSGA-II by the contribution of points to the hypervolume (HV) indicator. The HV is a performance indicator that measures convergence and maximum spread simultaneously. HV is the only unary indicator which is known to be Pareto-

[1] A unary indicator I is a function that assigns a real value to set of points $\mathcal{A} = \{\boldsymbol{a}^1, \ldots, \boldsymbol{a}^N\}$, where $\boldsymbol{a}^i \in \mathbb{R}^m$.

[2] Given $\boldsymbol{u}, \boldsymbol{v} \in \mathbb{R}^m$, $\boldsymbol{u}$ Pareto dominates $\boldsymbol{v}$ (denoted as $\boldsymbol{u} \prec \boldsymbol{v}$) if and only if $\forall i = 1, \ldots, m, u_i \leq v_i$ and there exists at least an index $j \in \{1, \ldots, m\} : u_j < v_j$.

compliant[3], but its use in MOEAs with many objectives is limited due to its high computational cost. In 2015, Menchaca-Méndez and Coello proposed an environmental selection mechanism based on the Generational Distance (GD) indicator [8] coupled with a diversity mechanism that adopts ϵ dominance to divide the objective space into hypercubes where the solutions are distributed. A clear disadvantage of GDE-MOEA is the determination of the ϵ value which is required to divide high-dimensional objective spaces and which has an impact on the generation of evenly distributed solutions. Finally, Δ_p-MOEA, proposed by Menchaca *et al.* [9], is an improvement of GDE-MOEA in which instead of using GD in its selection mechanism, adopts the Δ_p indicator. Δ_p-MOEA improves the diversity of the solutions produced, but it still depends on the calculation of the ϵ value to construct a reference set.

In order to overcome the difficulties of MOEAs that do not use weight vectors, we propose here an MOEA that takes advantage of the combination/synergy of the individual effect of two density estimators: one based on the IGD^+ indicator [10] and another one based on the Riesz s-energy indicator [11]. The main idea of our Evolutionary Multi-Objective Algorithm based on the Combination of the Riesz s-energy and IGD^+ (CRI-EMOA) is to analyze the convergence behavior during the search process in a statistical manner. If convergence stagnates, the generation of evenly distributed solutions is promoted using Riesz s-energy; otherwise, the IGD^+-based density estimator will drive the population to $\mathcal{PF}^*$.

The remainder of this paper is organized as follows. Section 2 provides some basic definitions. Our proposed approach is described in Section 3. Our experimental results are discussed in Section 4. Finally, Section 5 outlines our main conclusions and some possible paths for future work.

2 Background

In this work, we focus, without loss of generality, on unconstrained MOPs that *minimize* all the objective functions. A MOP is formally defined as follows:

$$\min_{\boldsymbol{x}\in\Omega} \boldsymbol{F}(\boldsymbol{x}) = (f_1(\boldsymbol{x}), f_2(\boldsymbol{x}), \ldots, f_m(\boldsymbol{x}))^T, \tag{1}$$

where $\boldsymbol{x} \in \Omega \subseteq \mathbb{R}^n$ is the vector of decision variables and Ω is the decision variable space. $f_i : \mathbb{R}^n \to \mathbb{R}, i = 1, 2, \ldots, m$ are the objective functions, where $m \geq 2$. MOPs having four or more objective functions are called many-objective optimization problems (MaOPs).

In the following, two unary quality indicators are described. For this purpose, let $\mathcal{A}$ represent an approximation to $\mathcal{PF}^*$ and $\mathcal{Z} \subset \mathbb{R}^m$ be a reference set. On the one hand, Ishibuchi *et al.* proposed the Inverted Generational Distance plus (IGD^+) indicator in 2015 [10]. This indicator measures the average distance between $\mathcal{Z}$ and $\mathcal{A}$, using a modified Euclidean distance that takes into account

[3] Let $\mathcal{A}$ and $\mathcal{B}$ be two non-empty sets of m-dimensional vectors and let I be a unary indicator. I is Pareto-compliant if and only if $\mathcal{A}$ dominates $\mathcal{B}$ implies $I(\mathcal{A}) > I(\mathcal{B})$ (assuming maximization of I).

Pareto dominance. Due to this modified distance, IGD^+ is a weakly Pareto compliant indicator. It is mathematically defined as follows:

$$\text{IGD}^+(\mathcal{A}, \mathcal{Z}) = \frac{1}{|\mathcal{Z}|} \sum_{\boldsymbol{z} \in \mathcal{Z}} \min_{\boldsymbol{a} \in \mathcal{A}} d^+(\boldsymbol{a}, \boldsymbol{z}), \tag{2}$$

where $d^+(\boldsymbol{a}, \boldsymbol{z}) = \sqrt{\sum_{k=1}^{m} \max(a_i - z_i, 0)^2}$ is the proposed modified Euclidean distance. On the other hand, Hardin and Saff proposed the Riesz s-energy indicator [11] in order to measure the even distribution of a set of points in d-dimensional manifolds. Its mathematical definition is given by:

$$E_s(\mathcal{A}) = \sum_{i \neq j} \|\boldsymbol{a}_i - \boldsymbol{a}_j\|^{-s} \tag{3}$$

where $s > 0$ is a fixed parameter that controls the degree of uniformity of the solutions in $\mathcal{A}$. Riesz s-energy has been found to lead to uniformly distributed point sets for the large class of rectifiable d-dimensional manifolds. Moreover, s is not a shape-dependent parameter [12].

3 Our Proposed Approach

Algorithm 1 CRI-EMOA general framework

Require: T_w, $\bar{\beta}$, $\bar{\theta}$
Ensure: Pareto front Approximation
Randomly initialize population P
$t \leftarrow 0$
while stopping criterion is not fulfilled **do**
  $q \leftarrow Variation(P)$
  $Q \leftarrow P \bigcup \{q\}$
  Normalize Q
  $\{L_1, L_2, \ldots, L_k\} \leftarrow$ nondominated-sorting(Q)
  $z_i^{\max} = \begin{cases} f_i^* = \max_{\boldsymbol{x} \in L_1} f_i(\boldsymbol{x}), & f_i^* > z_i^{\max} \\ z_i^{\max}, & \text{otherwise} \end{cases}$
  $S_{\text{HV}}[t \mod T_w] \leftarrow HV_{appr}(t)$
  Statistically analyze the last T_w samples in S_{HV} and generate β and θ
  if $k = 1$ and $\beta \leq \bar{\beta}$ and $\theta \in [-\bar{\theta}, \bar{\theta}]$ **then**
    $a_{\text{worst}} = \arg\max_{\boldsymbol{a} \in L_1} C_{E_s}(\boldsymbol{a}, L_1)$
  else
    if $|L_k| > 1$ **then**
      $a_{\text{worst}} = \arg\min_{\boldsymbol{a} \in L_k} C_{\text{IGD}^+}(\boldsymbol{a}, L_k, L_1)|$
    else
      a_{worst} is equal to the sole individual in L_k
  $P \leftarrow Q \setminus \{a_{\text{worst}}\}$
  $t \leftarrow t + 1$
return P

Quality indicators can be integrated into MOEAs in three different ways: 1) in the environmental selection mechanism, 2) as an update rule for archives, and 3) as density estimators (DEs). From these approaches, indicator-based DEs (IB-DEs) have been widely used. An IB-DE is the secondary selection mechanism of an MOEA. IB-DEs impose a total order among the solutions of an approximation set by calculating the individual contribution of each solution to the indicator value. Then, the worst-contributing solution is deleted from the population. In this work, we employed IGD^+ and Riesz s-energy as IB-DEs. Regarding IGD^+, the individual contribution C of a solution $\boldsymbol{a} \in \mathcal{A}$ is defined as follows: $C_{\text{IGD}^+}(\boldsymbol{a}, \mathcal{A}, \mathcal{Z}) = |\text{IGD}^+(\mathcal{A}, \mathcal{Z}) - \text{IGD}^+(\mathcal{A} \backslash \{\boldsymbol{a}\}, \mathcal{Z})|$. On the other hand, for Riesz s-energy, the individual contribution of $\boldsymbol{a} \in \mathcal{A}$ is given by: $C_{E_s}(\boldsymbol{a}, \mathcal{A}) = \frac{1}{2}[E_s(\mathcal{A}) - E_s(\mathcal{A} \backslash \{\boldsymbol{a}\})]$. On the basis of the above equations, IGD^+-DEs and E_s-DE are respectively defined as follows: (1) $a_{\text{worst}} = \arg\min_{\boldsymbol{a} \in \mathcal{A}} C_{\text{IGD}^+}(\boldsymbol{a}, \mathcal{A}, \mathcal{Z})$, and (2) $a_{\text{worst}} = \arg\max_{\boldsymbol{a} \in \mathcal{A}} C_{E_s}(\boldsymbol{a}, \mathcal{A})$, where a_{worst} denotes the solution having the wost-contributing value.

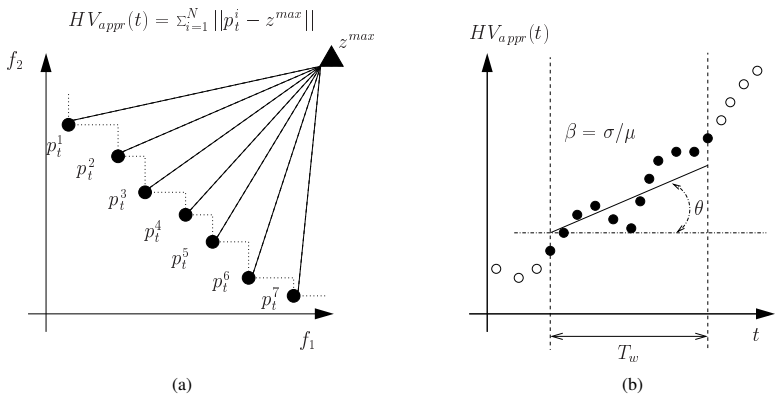

Fig. 1: (a) The Hypervolume approximation adds up all the distances between the reference point and each nondominated solution, (b) linear model of the convergence behavior created using the last T_w measures of HV_{appr}.

Algorithm 1 describes our proposed approach, called CRI-EMOA. It is a steady-state MOEA that adopts Pareto dominance in its environmental selection mechanism (using the nondominated sorting algorithm [6] in line 7) and an IB-DE as its secondary selection criterion. The main idea of CRI-EMOA is to exploit the properties of IGD^+ and Riesz s-energy by combining the individual effect of the corresponding IB-DEs. In other words, we want to drive the population towards the Pareto front using IGD^+-DE and, simultaneously, generating an evenly distributed approximation to the Pareto front through E_s-DE. To this end, CRI-EMOA switches between the two IB-DEs depending on a statistical analysis of the convergence behavior of the population, using an approximation to the hypervolume indicator (denoted as HV_{appr}). HV_{appr} is a simplification of

the proposal of Ishibuchi *et al.* [13] and it adds up all the distances between an anti-optimal reference point $\boldsymbol{z}^{\max}$ and the set of current nondominated solutions in L_1 (see Fig. 1a). In line 8, each $z_i^{\max}, i = 1, \ldots, m$ is updated if and only a worse objective value in L_1 is found and, then, $\mathrm{HV}_{\mathrm{appr}}(t)$ is computed such that the obtained value is stored in a circular array S_{HV} of size T_w. After the first T_w generations, S_{HV} will be full, and we can statistically analyze at each iteration the last T_w samples of $\mathrm{HV}_{\mathrm{appr}}$ as shown in Fig. 1b. In line 10, the mean μ and the standard deviation σ of the samples are computed such that the coefficient[4] of variation $\beta = \sigma/\mu$ is calculated. Additionally, the angle θ of a linear regression model of the samples is computed. Based on β and θ, we can exploit the properties of a certain IB-DE. If the number k of ranks produced by the nondominated sorting algorithm is equal to one and it holds that $\beta \leq \bar{\beta}$ and $\theta \in [-\bar{\theta}, \bar{\theta}]$ (where $\bar{\beta}$ and $\bar{\theta}$ are user-supplied parameters), it means that the convergence behavior is stagnated since there is not too much variation of $\mathrm{HV}_{\mathrm{appr}}$ and the linear model cannot be considered as ascending or descending. In consequence, we have to promote diversity using E_s-DE in line 12. Otherwise, if $|L_k| > 1$, IGD^+-DE is selected in line 15 in furtherance of improving the convergence of the population. In case $|L_k| = 1$, the sole individual in L_k is selected for elimination. Finally, the selected solution a_{worst} is deleted from the population, and a new generation is created.

4 Experimental Results

In this section, we analyze the performance of CRI-EMOA[5] when compared to several state-of-the-art MOEAs: NSGA-III [3], MOEA/D [2], MOMBI2 [4], Δ_p-MOEA [9] and GDE-MOEA [8]. The adopted MOEAs are classified into two main groups: MOEAs based on convex weight vectors and MOEAs not using convex weight vectors. NSGA-III[6], MOEA/D[7] and MOMBI2[8] belong to the first group while the remaining MOEAs[9] belong to the second group. We adopted MOPs from the DTLZ and WFG test suites, as well as from the minus versions of them, denoted as DTLZ^{-1} and WFG^{-1} that were proposed by Ishibuchi *et al.* [5]. The use of the minus versions of the benchmarks is to determine the performance of the considered MOEAs on MOPs whose Pareto fronts are not

[4] β is a standardized measure of dispersion that shows the extent of variability to the mean of the population.

[5] The source code of CRI-EMOA is available at `http://computacion.cs.cinvestav.mx/~jfalcon/CRI-EMOA.html`.

[6] We used the implementation available at: `http://web.ntnu.edu.tw/~tcchiang/publications/nsga3cpp/nsga3cpp.htm`.

[7] We used the implementation available at: `http://dces.essex.ac.uk/staff/zhang/webofmoead.htm`.

[8] We used the implementation available at `http://computacion.cs.cinvestav.mx/~rhernandez/`.

[9] The source code of Δ_p-MOEA and GDE-MOEA was provided by its author, Adriana Menchaca Méndez.

correlated to the simplex formed by a set of convex weight vectors. Additionally, the Pareto fronts of these MOPs cover a wide range of geometries such as linear, concave, degenerated, disconnected and mixed. In each case, we employed 3, 5 and 10 objective functions. In order to assess the performance of our proposed CRI-EMOA and the other MOEAs adopted in our comparative study, we applied HV and the Solow-Polasky indicator [14] for assessing convergence and diversity, respectively. For each MOEA in each test instance, we performed 30 independent executions.

4.1 Parameters settings

For a fair comparison, we set the population size N of all MOEAs, equals to the number of convex weight vectors that some of them employed, i.e., $N = C_{m-1}^{H+m-1}$, where m is the number of objective functions and H is a user-supplied parameter. Hence, in each case, the tuple (m, H, N) was set as follows: (3, 14, 120), (5, 5, 126), and (10, 3, 220). For the considered number of objective functions, we set $50{\times}10^3$, $70{\times}10^3$, and $120{\times}10^3$ function evaluations as our stopping criterion, respectively. Since our approach and all the considered MOEAs are genetic algorithms that use Simulated Binary Crossover and Polynomial-based Mutation as variation operators, we set the crossover probability (P_c), the crossover distribution index (N_c), the mutation probability (P_m), and the mutation distribution index (N_m) as follows. For MOPs having three objective functions $P_c = 0.9$ and $N_c = 20$, while for MaOPs $P_c = 1.0$ and $N_c = 30$. In all cases, $P_m = 1/n$, where n is the number of decision variables, and $N_m = 20$. Regarding both the WFG and the WFG^{-1} test problems with 3, 5 and 10 objectives, we set the number of variables as $n = 26, 30$ and 40, in each case using the following position-related parameters: 2, 4, and 9. Considering the DTLZ and DTLZ^{-1} instances, the number of variables is equal to $n = m + K - 1$, where $K = 5$ for DTLZ1 and DTLZ1^{-1}, $K = 10$ for DTLZ2, DTLZ5 and their minus versions, and $K = 20$ for DTLZ7 and DTLZ7^{-1}. For MOEA/D, the neighborhood size was set to 20 in all cases. Regarding CRI-EMOA, we employed $T_w = N$, $\bar{\beta} = 0.1$ and $\bar{\theta} = 0.25$ degrees for all instances.

4.2 Discussion of results

Tables 1 and 2 show the mean and standard deviation (in parentheses) obtained by all the compared algorithms for the hypervolume and the Solow-Polasky[10] indicators, respectively. The two best values among the MOEAs are highlighted using gray scale, where the darker tone corresponds to the best value. Aiming to obtain the statistical confidence of our results, we performed a one-tailed Wilcoxon test using a significance level of 0.05. Based on the Wilcoxon test, the symbol # is placed when CRI-EMOA performs better than another MOEA in a statistically significant way.

[10] The Solow-Polasky indicator requires a parameter θ that was set to 10.

Regarding the hypervolume indicator, CRI-EMOA is the best algorithm since it obtained the first place in 50% of the test problems. The second place corresponds to NSGA-III because it was the best MOEA in 8 out of 42 problems. However, it is worth emphasizing that for the minus benchmarks, NSGA-III only obtained one first place, specifically for DTLZ7^{-1} with 3 objective functions. In this regard, MOEA/D and MOMBI2 have just one first place in these minus benchmarks, and the remaining of their first places belong to the original DTLZ and WFG test suites. In consequence, it is clear the overspecialization of MOEAs using convex weight vectors on these benchmarks. Considering Δ_p-MOEA and GDE-MOEA, their performance is not so high. In fact, GDE-MOEA never obtains the first place and Δ_p-MOEA is the best algorithm in four test instances.

The Solow-Polasky indicator supports the good results of CRI-EMOA. This indicator measures the number of species present in the population. Thus, a larger value of the indicator is better because it means a good diversity of solutions. Our proposed approach produces well-distributed Pareto fronts in 26 out of 42 test instances (see Fig. 2). As a matter of fact, in most cases, when CRI-EMOA obtains the best HV value, it also obtains the best Solow-Polasky value. Hence, this a first insight that the synergy between IGD$^+$ and Riesz s-energy is actually responsible of its good performance in both convergence and diversity. Regarding the other MOEAs, NSGA-III and Δ_p-MOEA tie in second place since they obtained the best indicator value in 5 problems. Once again, NSGA-III can only produce good results for the original DTLZ and WFG problems. The worst algorithm regarding this indicator is MOMBI2.

For DTLZ1 and DTLZ1^{-1}, which have a linear Pareto front, CRI-EMOA does not obtain the best HV value. However, the Solow-Polasky indicator reflects that our approach has a better diversity. The top part of Fig. 2 shows the DTLZ1^{-1} fronts produced by all the MOEAs, and it is evident that CRI-EMOA produces an evenly distributed front in comparison with the adopted MOEAs. MOEA/D and MOMBI2 generate numerous solutions in the boundary of the front, while Δ_p-MOEA, GDE-MOEA and NSGA-III do not produce well-distributed solutions. For convex problems, i.e., DTLZ2^{-1} and DTLZ5^{-1}, it is evident that CRI-EMOA has a good performance. This is because it entirely covers the Pareto front, unlike the other MOEAs which are unable to do the same. This effect is illustrated in the second row of Fig. 2. For more complicated problems such as DTLZ7 and WFG2^{-1} that assess the ability of a MOEA to manage subpopulations, it is evident that CRI-MOEA produces better results. In the light of these results, we can claim that CRI-EMOA is a more general optimizer because its performance is not strongly linked to certain types of benchmark problems.

5 Conclusions and Future Work

In this paper, we propose an Evolutionary Multi-Objective Algorithm based on the combination of the Riesz s-energy and IGD$^+$ indicators. Our proposed approach, called CRI-EMOA, overcomes the overspecialization on certain bench-

Table 1: Mean and standard deviation (in parentheses) of the Hypervolume indicator. A symbol # is placed when CRI-EMOA performed significantly better than the other approaches based on a one-tailed Wilcoxon test using a significance level of $\alpha = 0.05$. The two best values are shown in gray scale, where the darker tone corresponds to the best value.

MOP	Dim.	CRI-EMOA	NSGA-III	MOEA/D	MOMBI2	Δ_p-MOEA	GDE-MOEA
DTLZ1	3	9.739039e-01 (3.858675e-04)	9.741141e-01 (3.120293e-04)	9.740945e-01 (2.619649e-04)	9.663444e-01# (1.080932e-03)	9.413310e-01# (1.964370e-02)	9.676446e-01# (2.362618e-03)
	5	9.877798e-01 (3.117917e-03)	9.986867e-01 (3.379577e-05)	9.986355e-01 (3.735697e-05)	9.904662e-01 (1.120127e-03)	3.320501e-02# (8.565974e-02)	4.840903e-01# (4.857106e-01)
	10	9.963635e-01 (1.065991e-03)	9.999939e-01 (2.139857e-06)	9.996746e-01 (1.025281e-04)	9.961538e-01 (9.574496e-04)	3.040882e-02# (5.310077e-02)	0.000000e+00# (0.000000e+00)
DTLZ2	3	7.419537e+00 (3.056980e-03)	7.421572e+00 (6.064709e-04)	7.421715e+00 (1.372809e-04)	7.380040e+00# (7.076656e-03)	7.371981e+00# (3.875638e-02)	7.350569e+00# (2.220661e-02)
	5	3.157090e+01 (2.415933e-02)	3.166721e+01 (6.548007e-04)	3.166781e+01 (5.129480e-04)	3.149886e+01# (2.619865e-02)	3.145814e+01# (6.277721e-02)	3.139858e+01# (7.085084e-02)
	10	1.021699e+03 (4.906893e-01)	1.023905e+03 (1.423610e-03)	1.023902e+03 (4.192719e-03)	1.022163e+03 (4.299615e-01)	1.022172e+03 (3.206973e-01)	8.223136e+02# (4.847301e+01)
DTLZ5	3	6.103498e+00 (2.913259e-04)	6.086240e+00# (3.462620e-03)	6.046024e+00# (2.227008e-04)	6.018466e+00# (3.166178e-03)	6.083103e+00# (4.024434e-02)	6.070736e+00# (4.307412e-02)
	5	2.306362e+01 (2.295313e-01)	2.162912e+01# (9.476133e-01)	2.328373e+01 (1.640165e-02)	2.175597e+01# (2.378197e-01)	2.152316e+01# (1.422545e+00)	1.943602e+01# (1.234198e+00)
	10	6.453781e+02 (4.080592e+01)	6.172582e+02# (4.132326e+01)	7.043390e+02 (1.714256e+00)	6.054385e+02# (4.091687e+01)	5.909772e+02# (7.644220e+01)	9.641241e+01# (1.554238e+01)
DTLZ7	3	1.634605e+01 (5.285233e-02)	1.631926e+01# (1.253568e-02)	1.620770e+01# (1.240925e-01)	1.613885e+01# (3.101462e-02)	1.612577e+01# (1.553168e-01)	1.615480e+01# (1.492618e-01)
	5	1.281085e+01 (1.974810e-01)	1.284401e+01 (3.182259e-02)	6.515913e+00# (1.170945e+00)	1.269646e+01# (4.907749e-02)	1.255217e+01# (1.341411e-01)	1.234590e+01# (2.234605e-01)
	10	3.479852e+00 (2.403388e-01)	1.806637e+00# (4.781492e-01)	2.756082e-03# (7.839814e-03)	3.033892e+00# (5.070947e-02)	3.027342e+00# (9.110566e-02)	2.080502e+00# (4.312007e-01)
WFG1	3	5.056544e+01 (1.657420e+00)	4.917540e+01# (1.742752e+00)	4.994533e+01 (2.615320e+00)	5.250059e+01 (1.702362e+00)	3.624458e+01# (9.571499e-01)	3.857628e+01# (9.613983e-01)
	5	4.509188e+03 (1.444159e+02)	4.049661e+03# (1.445036e+02)	4.522924e+03 (1.145447e+02)	4.682300e+03 (7.687667e+01)	3.198417e+03# (8.802857e+01)	3.499936e+03# (7.077142e+01)
	10	5.037589e+09 (8.535179e+07)	4.333786e+09# (4.767509e+07)	4.626119e+09# (9.082857e+07)	5.028893e+09 (6.062765e+07)	3.422833e+09# (2.182108e+07)	3.554077e+09# (4.491835e+07)
WFG2	3	1.000262e+02 (2.196919e-01)	1.000303e+02 (2.020421e-01)	9.425491e+01# (1.887090e+00)	9.995196e+01# (2.218338e-01)	2.860787e+01# (1.562061e-01)	2.878405e+01# (3.147546e-02)
	5	1.008420e+04 (5.737764e+01)	1.022660e+04 (2.444328e+01)	9.147103e+03# (2.989196e+02)	1.021265e+04 (2.425440e+01)	2.356563e+03# (1.302041e+01)	2.352252e+03# (2.298487e+01)
	10	1.348499e+10 (4.708062e+07)	1.343510e+10# (5.838755e+07)	1.153362e+10# (4.307707e+08)	1.346239e+10 (6.456777e+07)	2.433110e+09# (1.405830e+07)	2.417620e+09# (3.423298e+07)
WFG3	3	7.306197e+01 (3.258533e-01)	7.359113e+01 (3.698540e-01)	6.949014e+01 (2.043137e+00)	7.476737e+01 (2.010304e-01)	2.974536e+01 (2.198130e-01)	3.026476e+01 (9.539859e-02)
	5	6.735962e+03 (9.568603e+01)	6.705622e+03 (6.623165e+01)	5.831355e+03# (1.740491e+02)	6.720322e+03 (8.790247e+01)	2.425136e+03# (2.737458e+01)	2.467475e+03# (5.330311e+00)
	10	8.262095e+09 (2.467236e+08)	7.851751e+09# (1.420734e+08)	3.407782e+09# (4.406816e+08)	7.150575e+09# (8.942471e+08)	2.435088e+09# (7.572200e+07)	2.460728e+09# (2.651078e+07)
DTLZ1^{-1}	3	2.237019e+07 (1.096230e+05)	2.044422e+07# (2.230718e+05)	1.708422e+07# (2.776295e+05)	1.754720e+07# (1.024912e+04)	2.249206e+07 (9.308520e+04)	2.178413e+07# (1.919526e+05)
	5	5.990400e+10 (5.969126e+09)	1.653440e+10# (7.395153e+09)	1.275157e+10# (5.929635e+09)	1.829497e+10# (1.178680e+08)	8.421535e+10 (5.019922e+09)	7.834908e+10 (5.592427e+09)
	10	2.331601e+15 (1.332180e+15)	1.690928e+16 (1.594681e+16)	2.068669e+10# (2.776909e+10)	3.254959e+17 (7.964585e+16)	4.163772e+17 (1.784438e+17)	1.959914e+17 (7.692566e+16)
DTLZ2^{-1}	3	1.255756e+02 (1.372903e-01)	1.226427e+02# (4.332124e-01)	1.241646e+02# (1.767939e-01)	1.246298e+02# (1.975120e-02)	1.202429e+02# (1.235826e+00)	1.232392e+02# (4.384877e-01)
	5	1.823404e+03 (5.652832e+00)	1.529187e+03# (3.829295e+01)	1.570781e+03# (5.466206e+00)	1.377041e+03# (2.801096e+00)	1.615070e+03# (3.622796e+01)	1.684100e+03# (2.422012e+01)
	10	3.952305e+05 (6.000728e+03)	2.480210e+05# (3.215706e+04)	1.837497e+05# (3.540744e+03)	1.941735e+05# (4.318334e+03)	4.467775e+05 (1.153133e+04)	4.295481e+05 (1.104582e+04)
DTLZ5^{-1}	3	1.240446e+02 (1.543643e-01)	1.212729e+02# (4.506920e-01)	1.230132e+02# (1.173182e-01)	1.233805e+02# (2.897257e-02)	1.191790e+02# (1.218659e+00)	1.217996e+02# (3.913095e-01)
	5	1.830136e+03 (8.376583e+00)	1.526551e+03# (4.186892e+01)	1.532378e+03# (6.612506e+00)	1.490703e+03# (3.599646e+00)	1.550531e+03# (3.545733e+01)	1.663295e+03# (2.143198e+01)
	10	5.043244e+05 (5.933536e+03)	2.353908e+05# (2.658733e+04)	1.618586e+05# (2.870596e+03)	1.786897e+05# (4.650613e+03)	3.841427e+05# (1.267929e+04)	3.788162e+05# (1.409232e+04)
DTLZ7^{-1}	3	2.139263e+02 (1.705184e+00)	2.144482e+02 (1.844494e-02)	2.144785e+02 (3.401603e-03)	2.144350e+02 (1.484695e-02)	2.141398e+02 (6.446048e-01)	2.117720e+02# (5.620357e+00)
	5	1.193104e+03 (7.463449e+00)	1.190442e+03# (4.159670e+00)	6.388549e+02# (5.254422e+01)	1.197724e+03 (5.760920e+00)	1.195714e+03 (1.560565e+00)	1.167397e+03# (3.067229e+01)
	10	6.493424e+04 (1.799575e+02)	6.282093e+04# (1.236603e+02)	7.555843e+03# (6.397426e+02)	6.278498e+04# (5.606912e+02)	6.374490e+04# (1.597907e+02)	6.336153e+04# (1.579373e+02)
WFG1^{-1}	3	4.721465e+02 (5.118363e+01)	5.214593e+02 (2.613138e+01)	3.653092e+02# (2.305800e+00)	4.717969e+02# (4.848793e+01)	4.289752e+02# (4.089696e+01)	4.226979e+02# (4.328855e+01)
	5	8.957760e+04 (1.295509e+04)	6.766707e+04# (3.634016e+03)	4.312409e+04# (1.486578e+03)	8.604789e+04 (1.028243e+04)	6.687040e+04# (8.125469e+03)	5.398842e+04# (6.022448e+03)
	10	1.920711e+11 (1.254828e+10)	1.167307e+11# (9.811376e+09)	7.403214e+10# (3.748511e+09)	5.753336e+10# (1.586430e+09)	1.037099e+11# (5.197695e+09)	8.712812e+10# (9.507560e+09)
WFG2^{-1}	3	7.318853e+02 (4.584376e-01)	7.256549e+02# (2.471515e+00)	7.318071e+02# (5.137348e-01)	7.277336e+02# (7.218694e-01)	3.548073e+02# (4.631427e-01)	3.549143e+02# (1.951948e-01)
	5	1.638383e+05 (1.165835e+03)	1.470928e+05# (8.586496e+03)	1.122933e+05# (1.197256e+04)	1.499384e+05# (4.291788e+02)	4.315723e+04# (1.487567e+02)	4.156049e+04# (6.526206e+02)
	10	7.365072e+11 (6.254171e+09)	3.658776e+11# (1.973606e+10)	2.462168e+11# (2.934157e+10)	8.919695e+10# (1.091716e+10)	7.359311e+10# (2.277690e+08)	7.165991e+10# (8.580112e+08)
WFG3^{-1}	3	6.701244e+02 (9.728569e-01)	6.581207e+02# (2.461272e+00)	6.559404e+02# (1.399701e-01)	6.678986e+02# (4.368737e-01)	3.901185e+02# (2.837691e+00)	3.929122e+02# (1.663457e+00)
	5	1.460039e+05 (2.618698e+03)	1.271888e+05# (5.065268e+03)	9.818104e+04# (4.519958e+03)	1.345863e+05# (2.667741e+02)	4.822825e+04# (1.017141e+03)	4.912237e+04# (6.555485e+02)
	10	6.613123e+11 (2.015972e+10)	3.003925e+11# (2.070638e+10)	1.932277e+11# (2.123809e+10)	1.572410e+11# (3.994016e+09)	8.120430e+10# (2.177319e+09)	8.405921e+10# (1.518237e+09)

Table 2: Mean and standard deviation (in parentheses) of the Solow-Polasky indicator. A symbol # is placed when CRI-EMOA performed significantly better than the other approaches based on a one-tailed Wilcoxon test using a significance level of $\alpha = 0.05$. The two best values are shown in gray scale, where the darker tone corresponds to the best value.

MOP	Dim.	CRI-EMOA	NSGA-III	MOEA/D	MOMBI2	Δ_p-MOEA	GDE-MOEA
DTLZ1	3	9.944608e+00 (7.332450e-01)	9.394548e+00# (2.930251e-01)	9.314418e+00# (3.914884e-02)	9.000566e+00# (2.446366e-02)	7.811889e+00# (9.608413e-01)	9.208526e+00# (7.142910e-01)
	5	1.338590e+01 (5.394744e-01)	1.927839e+01 (2.200570e-01)	1.910784e+01 (2.012103e-01)	1.784107e+01 (5.535436e-02)	1.258001e+02 (3.614573e-01)	7.251588e+01 (4.806114e+01)
	10	1.785253e+01 (8.881198e-01)	4.215677e+01 (2.267717e+00)	3.557264e+01 (6.064497e-01)	3.493408e+01 (2.073537e+00)	2.196627e+02 (4.229255e-01)	1.937667e+02 (5.463117e+00)
DTLZ2	3	3.395527e+01 (9.380927e-02)	3.394704e+01# (1.377030e-02)	3.393654e+01# (1.057577e-03)	3.320388e+01# (3.200128e-02)	3.071966e+01# (5.648283e-01)	3.130480e+01# (3.907121e-01)
	5	9.880242e+01 (3.075202e+00)	1.023559e+02 (2.316020e-01)	1.017397e+02 (4.330518e-03)	1.000214e+02 (9.376416e-02)	9.047203e+01# (1.071667e+00)	8.885177e+01# (1.407456e+00)
	10	2.144437e+02 (8.333968e-01)	2.144143e+02# (4.461039e-02)	2.140218e+02# (1.052798e-02)	2.134074e+02# (2.440550e-01)	2.073661e+02# (1.076644e+00)	2.149790e+02 (1.820800e+00)
DTLZ5	3	8.835302e+00 (8.683488e-03)	8.689954e+00# (4.814112e-02)	4.565503e+01 (6.372947e-01)	8.446415e+00# (1.275105e-02)	8.725615e+00# (1.118233e-01)	9.131640e+00 (8.893988e-01)
	5	5.453458e+01 (3.836635e+00)	7.846618e+01 (3.806546e+00)	2.193721e+01# (7.192604e-01)	1.733111e+01# (1.215347e+00)	6.458870e+01 (4.414063e+00)	9.229364e+01 (3.153601e+00)
	10	1.426916e+02 (1.105651e+01)	1.855864e+02 (4.441145e+00)	7.636613e+00# (7.127440e-02)	2.097795e+01# (1.446842e+01)	1.636387e+02 (1.190412e+01)	2.009986e+02 (2.726407e+00)
DTLZ7	3	4.693189e+01 (4.563587e+00)	4.248938e+01# (8.838503e-01)	3.411613e+01# (6.885687e+00)	3.750968e+01# (4.295088e-01)	3.356066e+01# (8.918332e+00)	3.791999e+01# (1.074318e+01)
	5	7.703740e+01 (2.640331e+01)	9.605921e+01 (4.006295e+00)	2.595428e+01# (3.104755e-01)	7.335971e+01# (1.892378e+00)	1.014229e+02 (7.384253e+00)	8.467007e+01 (2.946531e+01)
	10	2.083721e+02 (1.401193e+01)	3.401405e+01# (4.627073e+01)	6.635493e+00# (8.377910e-01)	1.539631e+02# (1.794040e+01)	2.161036e+02 (1.887145e+00)	1.635677e+02# (5.659825e+01)
WFG1	3	6.266729e+01 (4.306665e+00)	5.624993e+01# (4.311929e+00)	5.053063e+01# (2.764405e+00)	5.406056e+01# (2.296813e+00)	3.936107e+01# (2.712236e+00)	4.901870e+01# (2.752851e+00)
	5	7.766310e+01 (9.797998e+00)	9.244372e+01 (7.266040e+00)	7.480740e+01 (3.832994e+00)	7.292172e+01# (5.425443e+00)	5.404634e+01# (4.708150e+00)	9.197836e+01 (4.116442e+00)
	10	1.153389e+02 (1.285140e+01)	8.917693e+01# (8.545945e+00)	1.552376e+01# (3.169355e+00)	6.819405e+01# (8.992674e+00)	9.420152e+01# (6.434297e+00)	1.681839e+02 (7.642626e+00)
WFG2	3	1.031961e+02 (6.913412e-01)	9.475339e+01# (5.942618e-01)	7.243218e+01# (1.099197e+00)	8.113447e+01# (1.694539e+00)	1.566893e+01# (4.695226e-01)	1.597100e+01# (5.210876e-01)
	5	9.923778e+01 (3.753788e+00)	1.259866e+02 (5.442239e-01)	9.750359e+01# (2.449040e+00)	1.226234e+02 (1.081329e+00)	2.491924e+01# (1.910851e+00)	2.346945e+01# (2.689896e+00)
	10	1.981494e+02 (4.297874e+00)	2.034942e+02 (6.167357e+00)	2.746068e+01# (9.314055e+00)	1.826284e+02# (2.286544e+01)	5.897645e+01# (4.305811e+00)	5.040485e+01# (7.890364e+00)
WFG3	3	7.979549e+01 (8.271398e-01)	5.447458e+01# (3.954759e+00)	6.745390e+01# (1.429561e+00)	4.359786e+01# (9.246690e-01)	2.088260e+01# (5.548807e-01)	2.237972e+01# (2.670741e-01)
	5	1.207901e+02 (1.514908e+00)	9.114798e+01# (4.803291e+00)	1.203892e+02# (1.120195e+00)	3.884532e+01# (5.191645e+00)	3.640185e+01# (1.590306e+00)	3.986356e+01# (1.669298e+00)
	10	2.198151e+02 (1.511883e-01)	1.842494e+02# (6.381996e+00)	1.685512e+02# (8.180955e-01)	1.223302e+02# (2.606946e+01)	7.655449e+01# (7.601122e+00)	9.569073e+01# (5.324356e+00)
DTLZ1^{-1}	3	1.238722e+02 (6.478345e-01)	1.192301e+02# (9.769981e-01)	1.110656e+02# (2.067972e-01)	1.076858e+02# (1.612270e+00)	1.194494e+02# (7.076038e-01)	1.026058e+02# (2.385964e+00)
	5	1.261138e+02 (3.746123e-01)	1.276049e+02 (7.483806e-01)	1.160278e+02# (3.018754e+00)	6.760143e+01# (4.891955e+00)	1.256546e+02# (4.961652e-01)	1.091644e+02# (2.978643e+00)
	10	2.200000e+02 (6.478398e-01)	2.194982e+02# (5.550208e-01)	1.845834e+01# (3.362045e+01)	2.177230e+02# (1.598879e+00)	2.199297e+02# (1.852502e-01)	1.956693e+02# (3.843626e+00)
DTLZ2^{-1}	3	1.129425e+02 (2.079720e-01)	9.168006e+01# (2.394444e+00)	9.466441e+01# (8.426911e-02)	9.433643e+01# (1.896075e-01)	8.857439e+01# (2.604729e+00)	8.818635e+01# (2.087133e+00)
	5	1.259981e+02 (4.099458e-04)	1.134723e+02# (2.970256e+00)	1.247875e+02# (1.631879e-01)	4.888021e+01# (1.111632e+00)	1.185054e+02# (1.679308e+00)	1.078721e+02# (2.347639e+00)
	10	2.249876e+02 (1.368722e+00)	2.075064e+02# (3.824826e+00)	2.079851e+02# (1.899257e+00)	1.810577e+02# (3.309000e+00)	2.118042e+02# (2.291510e+00)	1.931317e+02# (4.552358e+00)
DTLZ5^{-1}	3	1.069995e+02 (2.945855e-01)	8.469885e+01# (1.989703e+00)	7.942908e+01# (2.711812e-01)	8.622124e+01# (1.733700e-01)	8.484735e+01# (2.558670e+00)	8.305258e+01# (1.583665e+00)
	5	1.259747e+02 (3.780629e-03)	1.041424e+02# (3.722763e+00)	1.229014e+02# (1.837627e-01)	4.957223e+01# (1.976910e+00)	1.180479e+02# (1.846989e+00)	1.076183e+02# (2.710724e+00)
	10	2.199997e+02 (6.289321e-05)	1.579241e+02# (1.854156e+01)	1.997485e+02# (1.822188e+00)	1.636386e+02# (7.545337e+00)	2.094613e+02# (2.217251e+00)	1.946215e+02# (3.565477e+00)
DTLZ7^{-1}	3	2.345500e+01 (6.661044e+00)	2.375280e+01 (1.117994e+00)	2.588876e+01 (3.461387e+00)	1.994117e+01# (4.519640e-01)	2.178525e+01# (8.341601e-01)	1.805087e+01# (8.596927e+00)
	5	5.660901e+01 (1.568211e+01)	7.238636e+01 (1.269825e+01)	1.211841e+01# (1.172186e+00)	4.067053e+01# (9.192226e+00)	8.003609e+01 (3.156330e+00)	3.632242e+01# (3.834467e+01)
	10	2.043557e+02 (1.375176e+01)	1.347251e+01# (4.083423e+00)	4.293619e+00# (1.198274e-01)	8.812385e+00# (2.123041e+01)	2.008713e+02# (2.214667e+00)	2.028099e+02# (5.987172e+00)
WFG1^{-1}	3	6.415681e+01 (4.459890e+00)	5.511082e+01# (2.648385e+00)	1.663876e+01# (1.535080e+00)	4.730483e+01# (1.092483e+00)	4.842279e+01# (5.020350e+00)	4.279700e+01# (1.538301e+01)
	5	1.210334e+02 (2.192520e+00)	5.596308e+01# (5.654765e+00)	7.815456e+00# (1.225035e+00)	3.289189e+01# (2.858823e+00)	1.098994e+02# (4.122587e+00)	5.939438e+01# (3.673750e+01)
	10	2.186105e+02 (3.132639e-01)	6.927501e+01# (2.258115e+01)	2.480353e+00# (2.063527e+00)	3.476224e+01# (4.296041e+00)	1.950445e+02# (6.121614e+00)	1.138247e+02# (5.884228e+01)
WFG2^{-1}	3	1.140860e+02 (4.325357e-01)	9.532850e+01# (1.992380e+00)	8.890140e+01# (1.794800e-01)	9.018353e+01# (4.679018e-01)	3.230763e+00# (4.485117e-02)	2.757698e+00# (2.020626e-01)
	5	1.234346e+02 (7.027142e-01)	9.827363e+01# (2.826007e+00)	4.956629e+01# (8.529213e+00)	3.689443e+01# (1.559225e+00)	5.922537e+00# (7.879377e-01)	2.841850e+00# (6.498607e-01)
	10	2.196197e+02 (9.739353e-02)	2.001692e+02# (4.030917e+00)	2.500717e+01# (2.754994e+00)	1.075588e+02# (1.284360e+01)	1.138578e+01# (8.309404e-01)	7.783812e+00# (1.059255e+00)
WFG3^{-1}	3	1.075596e+02 (2.777510e-01)	7.484580e+01# (2.494935e+00)	6.164392e+01# (7.387154e-02)	7.097018e+01# (1.699291e-01)	2.303097e+01# (7.406376e-01)	2.381595e+01# (2.661523e-01)
	5	1.259055e+02 (2.786019e-02)	8.633630e+01# (4.246132e+00)	6.654930e+01# (3.739241e+00)	3.937358e+01# (1.177063e+00)	3.626087e+01# (2.423541e+00)	4.063424e+01# (2.006301e+00)
	10	2.199995e+02 (8.710466e-04)	1.929382e+02# (8.857025e+00)	5.251797e+01# (3.065445e+00)	1.414077e+02# (1.791224e+01)	7.135125e+01# (7.053632e+00)	9.336338e+01 (4.573319e+00)

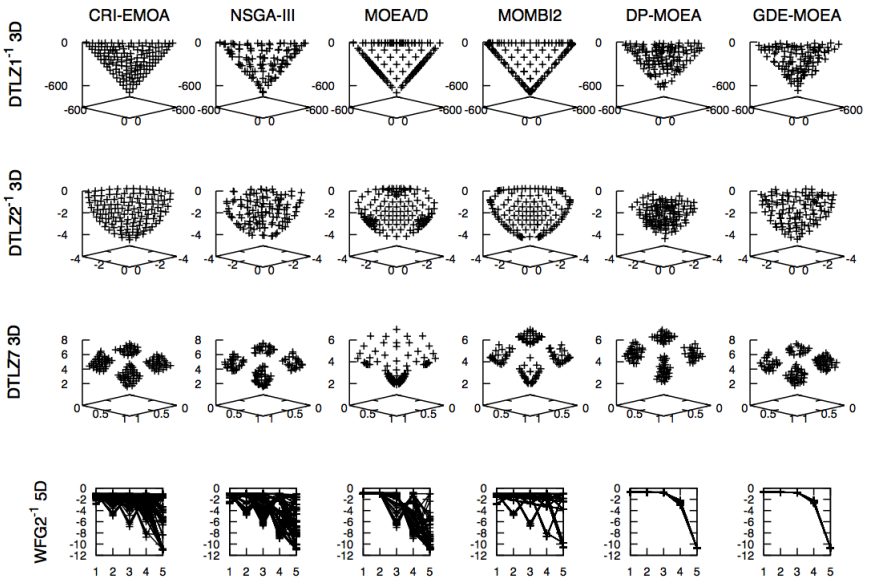

Fig. 2: Pareto fronts generated by CRI-EMOA and the adopted MOEAs. Each front corresponds to the median of the hypervolume value.

mark problems of state-of-the-art MOEAs that employ a set of convex weight vectors as search directions, as a reference set or as part of a quality indicator. CRI-EMOA exploits the convergence property of IGD^+ and promotes evenly distributed solutions using Riesz s-energy. Our proposal was compared with MOEAs with and without the use of convex weight vectors. Our experimental results showed that our approach has a competitive performance on the DTLZ and WFG instances, while it outperforms the adopted MOEAs on the $DTLZ^{-1}$ and WFG^{-1} problems. These empirical results provide some evidence about CRI-EMOA being a more general multi-objective optimizer. As part of our future work, we are interested in improving the performance of CRI-EMOA on the original benchmark problems while preserving its good performance on the minus versions of the considered test suites.

References

1. Carlos A. Coello Coello, Gary B. Lamont, and David A. Van Veldhuizen. *Evolutionary Algorithms for Solving Multi-Objective Problems*. Springer, New York, second edition, September 2007. ISBN 978-0-387-33254-3.
2. Qingfu Zhang and Hui Li. MOEA/D: A Multiobjective Evolutionary Algorithm Based on Decomposition. *IEEE Transactions on Evolutionary Computation*, 11(6):712–731, December 2007.
3. Kalyanmoy Deb and Himanshu Jain. An Evolutionary Many-Objective Optimization Algorithm Using Reference-Point-Based Nondominated Sorting Approach,

Part I: Solving Problems With Box Constraints. *IEEE Transactions on Evolutionary Computation*, 18(4):577–601, August 2014.
4. Raquel Hernández Gómez and Carlos A. Coello Coello. Improved Metaheuristic Based on the $R2$ Indicator for Many-Objective Optimization. In *2015 Genetic and Evolutionary Computation Conference (GECCO 2015)*, pages 679–686, Madrid, Spain, July 11-15 2015. ACM Press. ISBN 978-1-4503-3472-3.
5. Hisao Ishibuchi, Yu Setoguchi, Hiroyuki Masuda, and Yusuke Nojima. Performance of Decomposition-Based Many-Objective Algorithms Strongly Depends on Pareto Front Shapes. *IEEE Transactions on Evolutionary Computation*, 21(2):169–190, April 2017.
6. Kalyanmoy Deb, Samir Agrawal, Amrit Pratap, and T. Meyarivan. A Fast Elitist Non-Dominated Sorting Genetic Algorithm for Multi-Objective Optimization: NSGA-II. In Marc Schoenauer, Kalyanmoy Deb, Günter Rudolph, Xin Yao, Evelyne Lutton, Juan Julian Merelo, and Hans-Paul Schwefel, editors, *Proceedings of the Parallel Problem Solving from Nature VI Conference*, pages 849–858, Paris, France, 2000. Springer. Lecture Notes in Computer Science No. 1917.
7. Nicola Beume, Boris Naujoks, and Michael Emmerich. SMS-EMOA: Multiobjective selection based on dominated hypervolume. *European Journal of Operational Research*, 181(3):1653–1669, 16 September 2007.
8. Adriana Menchaca-Mendez and Carlos A. Coello Coello. GDE-MOEA : A New MOEA based on the Generational Distance indicator and ϵ-dominance. In *2015 IEEE Congress on Evolutionary Computation (CEC'2015)*, pages 947–955, Sendai, Japan, 25-28 May 2015. IEEE Press. ISBN 978-1-4799-7492-4.
9. Adriana Menchaca-Mendez, Carlos Hernández, and Carlos A. Coello Coello. Δ_p-MOEA: A New Multi-Objective Evolutionary Algorithm Based on the Δ_p Indicator. In *2016 IEEE Congress on Evolutionary Computation (CEC'2016)*, pages 3753–3760, Vancouver, Canada, 24-29 July 2016. IEEE Press. ISBN 978-1-5090-0623-9.
10. Hisao Ishibuchi, Hiroyuki Masuda, Yuki Tanigaki, and Yusuke Nojima. Modified Distance Calculation in Generational Distance and Inverted Generational Distance. In António Gaspar-Cunha, Carlos Henggeler Antunes, and Carlos Coello Coello, editors, *Evolutionary Multi-Criterion Optimization, 8th International Conference, EMO 2015*, pages 110–125. Springer. Lecture Notes in Computer Science Vol. 9019, Guimarães, Portugal, March 29 - April 1 2015.
11. D. P. Hardin and E. B. Saff. Discretizing Manifolds via Minimum Energy Points. *Notices of the AMS*, 51(10):1186–1194, 2004.
12. D. P. Hardin and E. B. Saff. Minimal Riesz energy point configurations for rectifiable d-dimensional manifolds. *Advances in Mathematics*, 193(1):174–204, 2005.
13. Hisao Ishibuchi, Noritaka Tsukamoto, Yuji Sakane, and Yusuke Nojima. Hypervolume Approximation Using Achievement Scalarizing Functions for Evolutionary Many-Objective Optimization. In *2009 IEEE Congress on Evolutionary Computation (CEC'2009)*, pages 530–537, Trondheim, Norway, May 2009. IEEE Press.
14. Michael T.M. Emmerich, André H. Deutz, and Johannes W. Kruisselbrink. On Quality Indicators for Black-Box Level Set Approximation. In Emilia Tantar, Alexandru-Adrian Tantar, Pascal Bouvry, Pierre Del Moral, Pierrick Legrand, Carlos A. Coello Coello, and Oliver Schütze, editors, *EVOLVE - A bridge between Probability, Set Oriented Numerics and Evolutionary Computation*, chapter 4, pages 157–185. Springer-Verlag. Studies in Computational Intelligence Vol. 447, Heidelberg, Germany, 2013. 978-3-642-32725-4.